The influence of the initial velocity on the anomalous wave dynamics in expanding fireball

The influence of the initial velocity on the anomalous wave dynamics in expanding fireball

A V Konyukhov and A P Likhachev

Joint Institute for High Temperatures of the Russian Academy of Sciences, Izhorskaya 13 Bldg 2, Moscow 125412, Russia

E-mail: konyukhov_av@mail.ru

Abstract. The quark–gluon plasma fireball expansion, appearing in the collision of relativistic heavy ions, can be accompanied by the wave anomalies associated with the quark–hadron phase transition. Namely, the composite rarefaction wave, which includes the rarefaction shock, can arise instead of a simple rarefaction wave. The emphasis of the given work is focused on the special features of these wave processes induced by nonzero quark–gluon plasma velocity at the beginning of the hydrodynamic stage of the fireball expansion. The simulation has been conducted in the framework of relativistic hydrodynamics. The equation of state used is based on the variant of the MIT-bag model. The initial conditions are formulated under the assumption that the distributions of the energy density and the baryon number density are uniform, while the radial velocity changes linearly from zero at the center to the assigned value at the fireball border. The results of the calculations have shown the strong dependence of the wave phenomena observed on the initial velocity distribution.

1. Introduction

The collision of relativistic heavy ions is the multi-stage process with the different dominant physics at each stage (see, e.g., [1,2]). The model describing this process entirely must be multi-module and is still missing [3]. It forces to consider the stages separately under models that meet the current knowledge about their physics. The hydrodynamic approach is recognized to be valid to describe the quark–gluon plasma (QGP) fireball expansion after the QGP thermalization and up to the final kinetic freeze-out. The comprehensive review of works used this approach in various model modifications and with different research goals is given, e.g., in [3, 4]. In a special way it should be note publications [5–8], in which the specific features of the fireball expansion wave dynamics were considered. These features are connected with the quark–hadron phase transition (QGPT). As it is known (see, e.g., [9]), the Poisson adiabat, passing through the phase transition region, has kinks at the points of intersection with phase interfaces and becomes not convex. The Riemann problem solution in relation to the present case gives the rarefaction wave in the QGP, the rarefaction shock, and the rarefaction wave in the hadronic gas (HG) instead of a simple rarefaction wave. The region of a constant solution (plateau) appears between the rarefaction wave in the QGP and the rarefaction shock. The plateau parameters correspond to pre-shock state. It should be note that the two-phase state is present within the internal structure of the rarefaction shock only.

The hydrodynamic calculation makes it possible to estimate the energy density and temperature in the HG phase formed in the approximation of the instantaneous kinetics of

the phase transition, which potentially ensures the relation between the equation of state of nuclear matter and the experimental data. The experimental detection of the elements of a combined rarefaction wave (plateau and rarefaction shock) not only will be an unconditional signal of the phase transition from the QGP to the HG but also could be used for quantitative refinement of the equation of state.

The research presented is motivated by the following consideration. One of the main problems of the hydrodynamic description of the fireball expansion stage is the choice of the initial conditions. At the moment, the information on the parameter distributions at the end of thermalization process remains quite uncertain and contradictory. Typically, this problem is solved with the involvement of additional, often intuitive assumptions based, for instance, on the classical scenarios of the collision process [10] or later model considerations (see, e.g., [3,11]). Obviously, under these circumstances inexactness in initial conditions is possible and even inevitable. In this context, the choice of the initial conditions is of particular importance for the correct prediction of the wave dynamics of the QGP fireball expansion. The study of this problem is the main goal of this work.

2. Preliminary consideration

As mentioned above, the hydrodynamic description used to model collective behavior of reaction products has essentially limited time range of applicability. The initial stage of the nuclei collision is suggested to be reaction, in which only separate partons are involved. It is assumed that after some temporal interval an ensemble of particles produced by the reaction achieves the local thermodynamic equilibrium predicted by the statistical theory. This interval is estimated as $(0.1\text{–}0.2)R/c$ [1, 12], where R is the nucleus characteristic size, c is the speed of light. With the completion of the thermalization the hydrodynamic model is supposed to be applicable.

Several formulations of initial conditions needed for hydrodynamic simulation have been developed (see, for example, reviews [3, 4]). Mainly, these formulations suppose that the expansion of the QGP fireball begins from the state of rest with zero velocity everywhere inside fireball. It seems to be very strong assumption. To the moment of thermalization, the velocity of particles has some distribution, because during the initial non-hydrodynamic stage the medium is relatively transparent and the concentration of fast-moving particles with directed outward velocity increases with the distance from the center; obviously, the average velocity directly in the fireball center is zero from the symmetry condition.

Here we are comparing solutions with zero and linearly increasing initial velocities. The calculations are carried out in the 1+1 and 2+1 formulations described below. For the sake of simplicity the initial baryon number and energy densities inside the QGP fireball are suggested to be uniform. Of course, the latter as well as the linear character of the initial velocity distribution are only assumptions taken to facilitate the detection of the sensitivity of the solution wave structure to such a change in the velocity initial condition.

3. Equations

The equations of relativistic fluid dynamics include the energy-momentum conservation equation

$$\nabla_\beta T^{\alpha\beta} = 0, \tag{1}$$

∇_β is covariant derivative in space-time; energy momentum tensor is given by

$$T^{\alpha\beta} = (e + p)u^\alpha u^\beta - g^{\alpha\beta} p,$$

where e and p are the energy density and pressure defined in the rest coordinate system; the metric tensor (for special theory of relativity) is $g^{\alpha\beta} = \mathrm{diag}(1, -1, -1, -1)$, $u^\alpha = (\Gamma, v\Gamma)^T$ is the

4-velocity; $\Gamma = 1/(1-v^2)^{1/2}$ is the Lorentz factor (the units are used in which the speed of light is 1) [13].

The system is complemented by the conservation low for the net baryon number

$$\nabla_\alpha (n u^\alpha) = 0. \tag{2}$$

4. Numerical method

The set of equations (1)–(2) can be represented in the form of hyperbolic conservation laws in the Cartesian coordinates (t, x, y):

$$\frac{\partial U}{\partial t} + \frac{\partial F^1(U)}{\partial x} + \frac{\partial F^2(U)}{\partial y} = 0, \tag{3}$$

where $U = (D, S^1, S^2, \tau)^T$ is the vector of conservative variables, the fluxes of which have the form $F^i = (Dv^i, S^1 v^i + p\delta^{1i}, S^2 v^i + p\delta^{2i}, S^i - Dv^i)^T$. The conservative variables D, S^1, S^2 and τ are related to the baryon number density, 3-velocity components and relativistic enthalpy h=1+(e+p)/n by the following relations

$$D = n\Gamma, \quad S^i = nh\Gamma^2 v^i, \quad \tau = nh\Gamma^2 - p - n\Gamma. \tag{4}$$

The equations where solved iteratively for the primitive variables at each cell interface.

The equation system (2) is hyperbolic. The right eigenvectors for the Jacobian matrix $\partial F_n/\partial U$, $F_n = F^1 n_x + F^2 n_y$, are as follows

$$\begin{aligned}
\mathbf{r}^1 &= \left(\tfrac{k}{h\Gamma(k-1)} \quad v_x, \quad v_y, \quad 1 - \tfrac{k}{h\Gamma(k-1)} \right)^T, \\
\mathbf{r}^2 &= \left(v_y\Gamma, \quad 2h\Gamma^2 v_t v_x - hn_y, \quad 2h\Gamma^2 v_t v_y + hn_x, \quad -v_t\Gamma + 2hv_t\Gamma^2 \right)^T, \\
\mathbf{r}^3 &= \left(1, \quad (-n_y v_t + n_x \tfrac{\lambda_m}{a_m})h\Gamma, \quad (n_x v_t + n_y \tfrac{\lambda_m}{a_m})h\Gamma, \quad -1 + \tfrac{h\Gamma}{a_m} \right)^T, \\
\mathbf{r}^4 &= \left(1, \quad (-n_y v_t + n_x \tfrac{\lambda_p}{a_p})h\Gamma, \quad (n_x v_t + n_y \tfrac{\lambda_p}{a_p})h\Gamma, \quad -1 + \tfrac{h\Gamma}{a_p} \right)^T.
\end{aligned} \tag{5}$$

The variations of the local characteristic variables are defined at the cell faces by the equations

$$\begin{aligned}
\alpha_1 &= \Gamma(k-1)(h\,\Delta D + \Gamma(v \cdot \Delta S - \Delta D - \Delta\tau)), \\
\alpha_2 &= \frac{v_t}{h(1-v_n^2)}\,(v_n \Delta S_n - \Delta D - \Delta\tau) + \frac{1}{h}\Delta S_t, \\
\alpha_3 &= +\frac{a_m}{h\Gamma(\lambda_p - \lambda_m)}[(v_n - \lambda_p)\Lambda - (a_p + v_n b_p)\Delta S_n + (b_p + v_n a_p)(\Delta D + \Delta\tau)], \\
\alpha_4 &= -\frac{a_p}{h\Gamma(\lambda_p - \lambda_m)}[(v_n - \lambda_m)\Lambda - (a_m + v_n b_m)\Delta S_n + (b_m + v_n a_m)(\Delta D + \Delta\tau)].
\end{aligned} \tag{6}$$

In (5) and (6) the following notations are used:

$$\Lambda = \Gamma\left((k-1)h\,\Delta D + (k+1)\Gamma(v \cdot \Delta S - \Delta D - \Delta\tau)\right), \quad b_l = \frac{v_n - \lambda_l}{1 - v_n^2}, \quad a_l = \frac{1 - v_n\lambda_l}{1 - v_n^2}.$$

Here, $l = m,\ p$; v_n, v_t, S_n, S_t are normal and tangential components of the 3-velocity and momentum density; Δf denotes jump of the variable f at the interface. The eigenvalues of the Jacobian matrix are

$$\begin{aligned}
\lambda_1 &= \lambda_2 = v_n, \\
\lambda_3 &= \lambda_m = \frac{v_n(1-c^2) - A\sqrt{(1-v^2)[1 - v^2c^2 - v_n^2(1-c^2)]}}{1 - v^2c^2}, \\
\lambda_4 &= \lambda_p = \frac{v_n(1-c^2) + A\sqrt{(1-v^2)[1 - v^2c^2 - v_n^2(1-c^2)]}}{1 - v^2c^2},
\end{aligned} \tag{7}$$

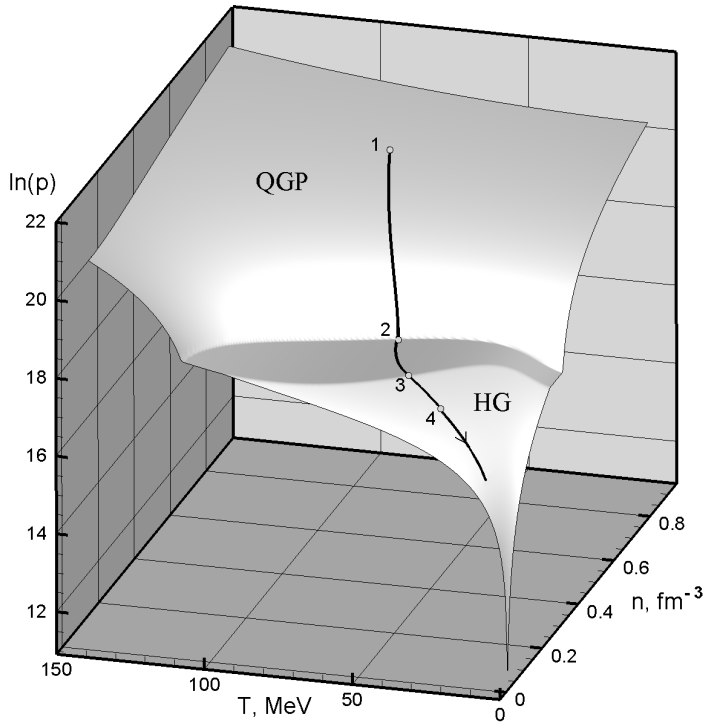

Figure 1. Phase diagram in p–T–n variables (n is baryon number density). The Poisson adiabat passes through the initial state of the QGP fireball (point 1) and intersects the QGPT region interfaces at points 2 and 3. Points 2 and 4 are the pre- and post-rarefaction-shock states. Notice that the point 4 practically lies on the primary isentrope, i.e. the entropy change in the rarefaction shock is rather small.

where the relativistic speed of sound is defined by

$$c^2 = \left(\frac{\partial p}{\partial e}\right)_s = \left(\frac{\partial p}{\partial e}\right)_n + \frac{n}{p+e}\left(\frac{\partial p}{\partial n}\right)_e, \qquad k = \frac{h}{h - (\partial e/\partial n)_p}. \tag{8}$$

To calculate flow variables at cell interfaces, the third order accuracy essentially non-oscillatory (ENO) scheme [14] has been used. The numerical flux vector at the Gaussian integration points at the interfaces has been determined using HLLC approximate Riemann solver [15]. The high resolution in time was provided using the third order accuracy Runge–Kutta TVD preserving scheme [14].

5. Results

The EOS of subhadronic matter built on the basis of the variant of the MIT-bag model [16] has been used. This EOS describes the QHPT clearly visible in the phase diagram (see figure 2). The QGP fireball expansion with zero and linearly increasing initial velocities has been considered. The simulation has been carried out in the 1+1 (the expansion of the plane layer and circular cylinder) and the 2+1 (the expansion of elliptical cylinder) formulations. In all calculations the initial distributions of thermodynamic parameters inside the QGP fireball are uniform: $p = 10^9$ MeV^4, $T = 75$ MeV, $n = 0.561$ fm^{-3}. These values correspond to point 1 in figure 2. In the space, surrounding the QGP fireball, the baryon number density and the pressure are

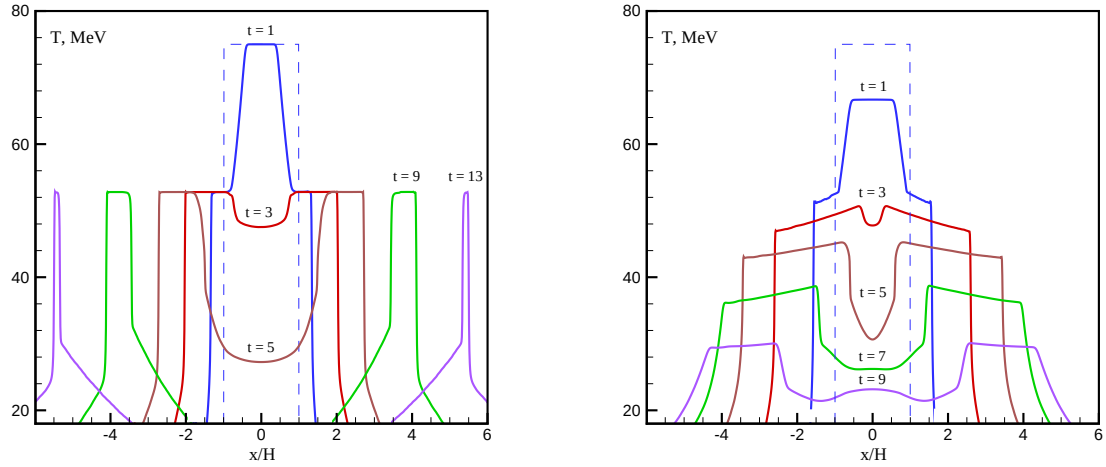

Figure 2. Spatial temperature distributions at successive instants: the QGP layer expansion with zero (left panel) and linearly increasing (right panel) initial velocity. Here and in figures 4–6 curve numbers denote dimensionless time; the dashed line shows the initial parameter distribution.

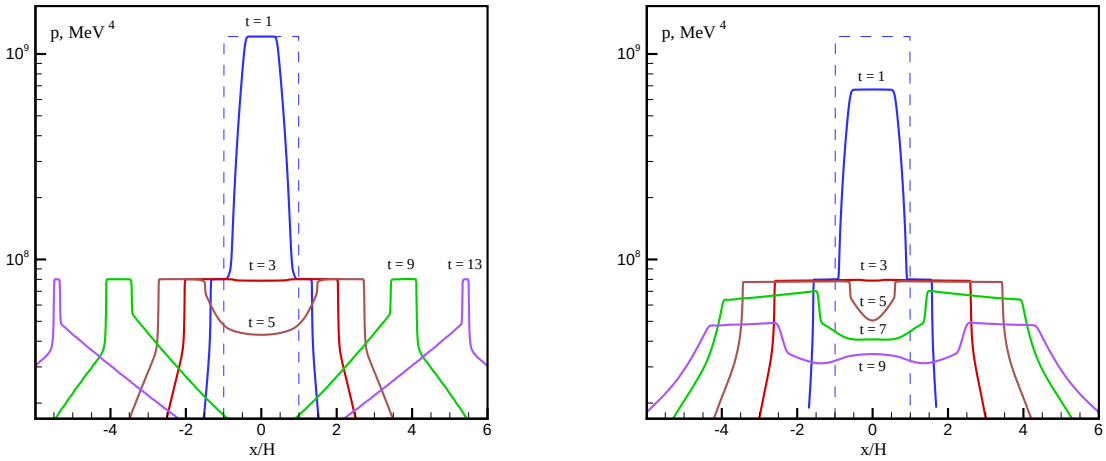

Figure 3. Spatial pressure distributions at successive instants of time: the QGP layer expansion with zero (left panel) and linearly increasing (right panel) initial velocity.

assumed to be 10^{-3} of their values within the QGP fireball to model the vacuum in numerical solutions.

Consider the results of numerical solutions. The evolution of the plane QGP layer expansion (the 1+1 formulation) is presented in figures 2–4. In the case of the nonzero initial velocity inside the QGP layer it has been assigned as $u(x) = U_0 x/H$, where H is the initial layer thickness, $U_0 = 0.3$ is the velocity at the layer border referred to the speed of light.

The solution with the zero initial velocity is shown in the left panels of figures 2–4. Until the reflection of the rarefaction wave in the QGP phase from the plane of symmetry, the solution

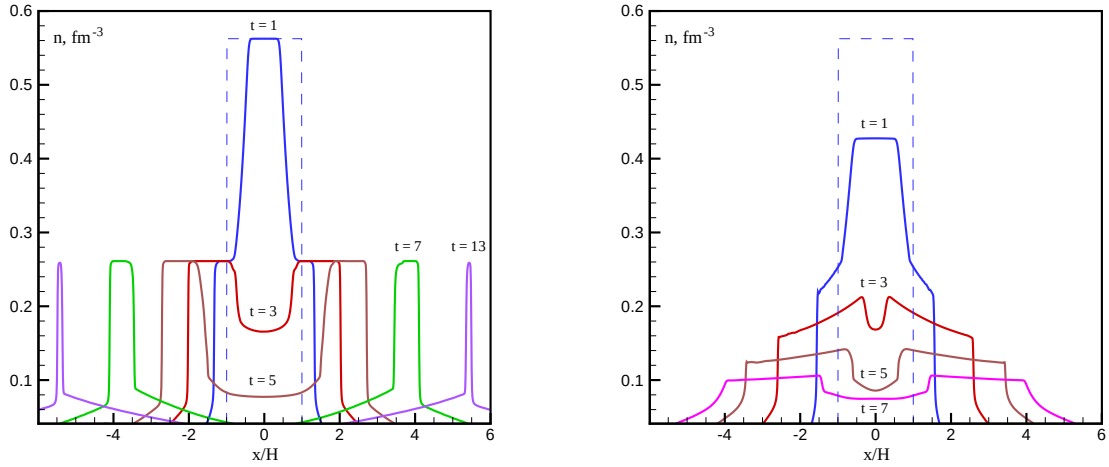

Figure 4. Spatial baryon number density distributions at successive instants of time: the QGP layer expansion with zero (left panel) and linearly increasing (right panel) initial velocity.

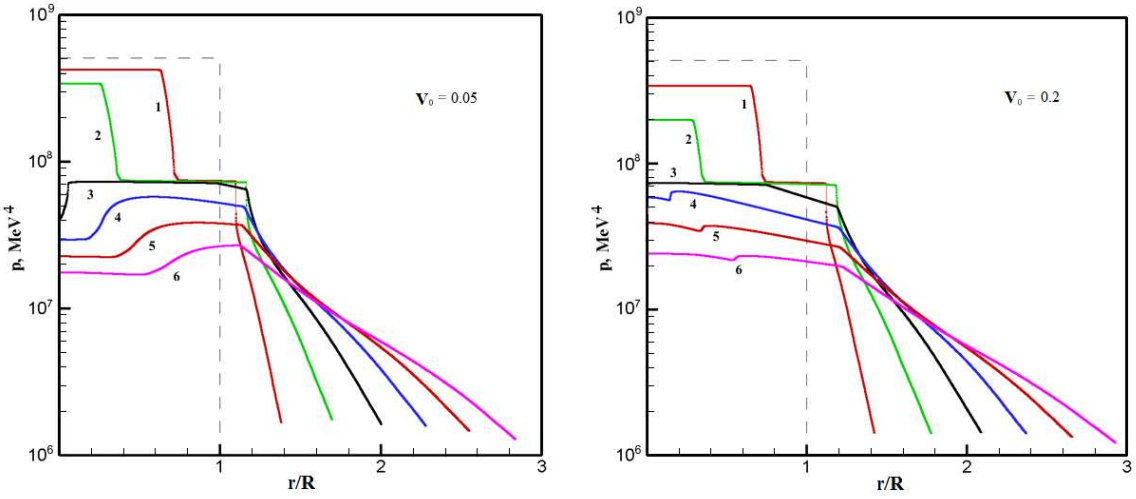

Figure 5. Spatial pressure distributions at successive instants: the QGP circular cylinder expansion with $V_0 = 0.05$ (left panel) and $V_0 = 0.2$ (right panel). The dashed line shows the initial pressure distribution.

is self-similar and qualitatively corresponds to the example described above in the introduction. After the formation of the reflected rarefaction wave the solution becomes more complicated. The pressure distribution has minimum in the layer centre, which decreases with time. When parameters of the expansion reach the point 2 in figure 1 (the two-phase region interface), the rarefaction wave transforms into the composite rarefaction wave, also including the rarefaction shock. The two-phase matter is presented within the internal structure of the rarefaction shocks and a short time in the central part of the layer when parameters behind the reflected rarefaction wave are between points 2 and 3 (figure 1). The pure QGP state in the expanding matter does not exist after the merging of rarefaction shocks.

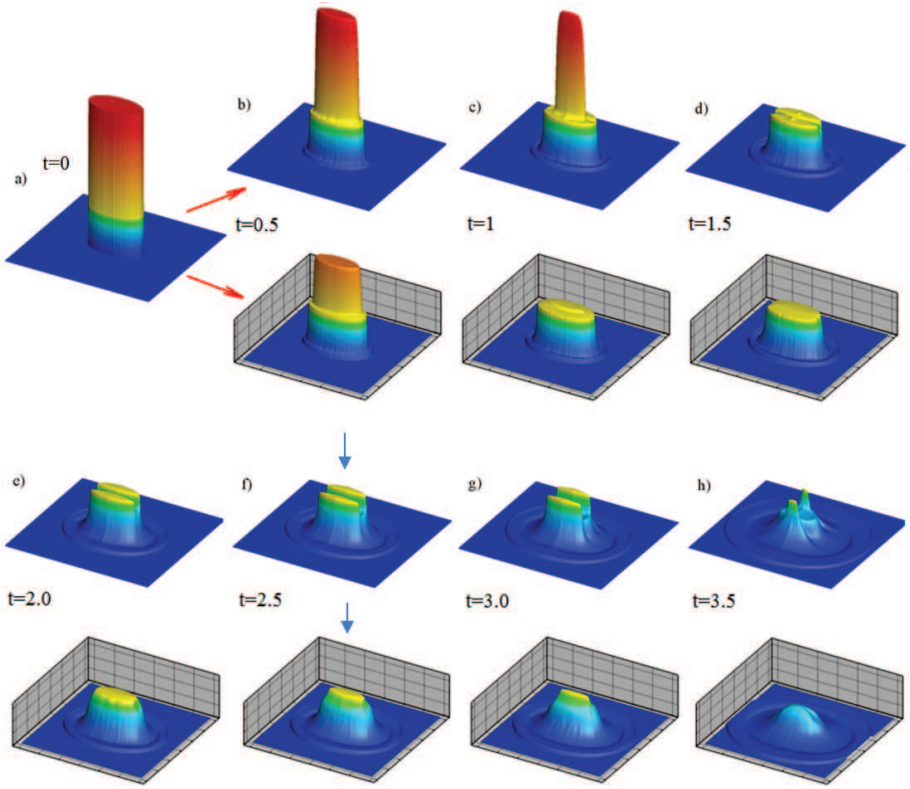

Figure 6. Spatial pressure distributions at successive instants: the QGP elliptical cylinder expansion without (upper row) and with (lower row) initial expansion velocity. Color reflects approximately the phase state of matter: "red" is the QGP, "blue" is the HG, "yellow" is the two-phase region.

The solution with non-zero initial velocity shown in the right panels of figures 2–4 is markedly different from that considered above. The expansion begins immediately throughout the volume of the layer; the self-similar stage is absent. The lifetime of a pure QGP state becomes much less and at a chosen value of V_0 is approximately limited by the moment of the rarefaction wave reflection from the plane of symmetry. The "plateau" between the rarefaction wave in the QGP phase and the rarefaction shock is replaced by weakly-gradient region. The two-phase matter can be presented in this region as well as within the internal structure of the rarefaction shocks.

Let us consider the QGP circular cylinder expansion (the 1+1 formulation). The initial radial velocity is assigned as $v_r(r) = V_0 r/R$, where R is the initial cylinder radius. V_0 is the initial velocity at the cylinder border referred to the speed of light. Calculations with $V_0 = 0.05$ and $V_0 = 0.2$ have been performed. The simulation results are presented in figure 5.

In the beginning of the expansion process the composite rarefaction wave is formed (curve 1 and 2). The rarefaction shock, being a wave of phase transition, separates the matter in the QGP (high pressure region) and HG (low pressure region) states. The pressure on the left of the rarefaction wave decreases with time due to adiabatic expansion caused by the presence of the initial expansion velocity. The converging expansion wave is reflected from the axis of symmetry. The reflected diverging expansion wave may be composite, if it passes through the two-phase matter for a time sufficient for formation of the expansion shock. Otherwise, the composite expansion wave is not formed (e.g., curves 4–6, the reflected wave passes through the HG matter only). In this case, the lifetime of the QGP, being an important parameter of

the diagnostics of the QGPT, is determined by the moment of the converging rarefaction wave reflection from the axis of symmetry.

The solutions obtained differ from the case of the zero initial velocity by the faster QGP expansion, which, in addition, begins immediately throughout the volume of the cylinder. The distinctions become more pronounced with increasing V_0. In particular, at $V_0 = 0.05$ the rarefaction wave in the QGP is reflected from the axis of symmetry with formation of the perceptible expansion shock (curve 3 in the left panel). At $V_0 = 0.2$ the reflected shock has a very short lifetime and poorly visible. It should be noted that the solution with $V_0 = 0.05$ (left panel of figure 5) has much in common with the QGP layer expansion with non-zero initial velocity (right panel of figure 4).

Finally consider the QGP elliptical cylinder expansion (the 2+1 formulation). The problem has been solved in two formulation: with expansion from the state of rest and with initial velocity assigned as $v(x, y) = 0.1(x/a, y/b)$, where a and b are the ellipse axes, $a/b = 2$. The simulation results are presented in figure 6.

As one can see in figure 6, the pressure distributions have plateau-like regions corresponding to the matter two-phase state. The two-phase state lifetime is more than that for the QGP. That is why the evolution of the shape of the two-phase region and the velocity distribution within it are important. Taking into account this fact, the following feature of the solutions should be noted. In the case of expansion with a nonzero initial velocity the two-phase region is located in the vicinity of the fireball centre. In the case of zero initial velocity the fragmentation of the two phase region takes place. The fragments are located on the fireball periphery and therefore have a greater (close to the speed of light) velocities in the laboratory frame. The last demonstrates strong dependence of anomalous wave phenomena caused by the presence of the QGPT on the initial velocity condition.

6. Conclusion

The influence of the initial velocity on the wave structure of the fireball expansion has been studied. The calculations have been performed using the equation of state for hot nuclear matter, which describes the QGPT. The specific wave phenomena caused by the imposition of the initial velocity of the QGP fireball expansion have been analyzed in different formulations. The wave structure of the solution is shown to depend strongly on the presence of initial expansion. At the same time it is found that in all formulations the pressure distribution has plateau-like region corresponding to the matter two-phase state. This feature is preserved for a rather long time and may be a signal of the QGPT together with the formation of the rarefaction shock.

Acknowledgments

The work is supported by the Russian Foundation for Basic Research (grant 16-02-01179). The authors are grateful to I L Iosilevskiy and P R Levashov for fruitful discussions.

References

[1] Fortov V E 2013 *Physics of High Energy Densities* (Moscow: FIZMATLIT)
[2] Shuryak E 2009 *Prog. Part. Nucl. Phys.* **62** 48–101
[3] Nonaka C and Asakawa M 2012 *Prog. Theor. Exp. Phys.* 01A208
[4] de Souza R D, Koide T and Kodama T 2016 *Prog. Part. Nucl. Phys.* **86** 35–85
[5] Bugaev K A, Gorenstein M I, Kampfer B and Zhdanov V I 1989 *Phys. Rev.* D **40** 2903–2913
[6] Bugaev K A, Gorenstein M I and Rischke D 1990 *Phys. Rev.* D **52** 1121–1123
[7] Bugaev K A, Ivanytskyi A I, Oliinychenko D R, Sagun V V, Mishustin I N, Rischke D H, Satarov L M and Zinovjev G M 2015 *Phys. Part. Nucl. Lett.* **12** 238–245
[8] Konyukhov A V and Likhachev A P 2015 *J. Phys.: Conf. Ser.* **653** 012076
[9] Zeldovich Ya B and Raizer Yu P 1967 *Physics of Shock Waves and High-Temperature Hydrodynamic Phenomena* (New York: Academic Press)

[10] Bjorken B D 1983 *Phys. Rev.* D **27** 140–151
[11] Petersen H and Bleicher M 2009 *Phys. Rev.* C **79** 054904
[12] Roizen I I, Feinberg E L and Chernavskaya O D 2004 *Phys. Usp.* **47** 427–446
[13] Landau L D and Lifshitz E M 1987 *Fluid Mechanics* 2nd ed (Oxford: Pergamon)
[14] Shu C W 1998 *Advanced Numerical Approximation of Nonlinear Hyperbolic Equations* (Berlin, Heidelberg) pp 325–432
[15] Mignone A and Bodo G 2005 *Mon. Not. R. Astron. Soc.* **364** 126–136
[16] Cleymans J, Redlich R V and Suhonen E 1986 *Phys. Rep.* **130** 217–292